EXPERIMENTAL STUDY ON PHASE DISTRIBUTION AND HEAT TRANSFER OF DISPERSED TWO-PHASE FLOW IN CURVED CHANNELS

F. Mayinger and M.J. Wang
Lehrstuhl A für Thermodynamik, T.U. München, 8000 München 2, FRG

Abstract

An experimental study on phase distribution and heat transfer of the dispersed two-phase flow in 90 deg bends is presented. Remarkable heat transfer augmentation, especially at the outer side of bends is confirmed. As revealed by measurement, this behavior of the flow is due mainly to the change of phase distribution. For analysis of dispersed flow heat transfer in the curved channel, contributions from both the vapor convection and the droplet-wall impact should be taken into account.

Nomenclature

A_i	area in cross-section	m^2
C	capacitor	F
D	tube diameter	m
De	Dean number	-
F_i	liquid distribution factor	-
Fr	Froude number	-
g	gravitational acceleration	m/s^2
G	mass flow rate	kg/m^2s
h	heat transfer coefficient	kW/m^2K
R_c	bend radius	m
R_t	tube radius	m
Re	Reynolds number	-
P	pressure	bar
$\dot{q}_w$	heat flux	kW/m^2
T	Temperature	K (°C)
V_m	mean velocity	m/s
x	real vapor quality	-
$x_{e,i}$	inlet vapor equilibrium quality	-

Greek symbols

α	void fraction	-
β	bend angle	deg
ε	dielectric constant	-
μ	dynamic viscosity	kg/ms
ϱ	density	kg/m^3

Subscripts

cr	critical
f	liquid
g	vapor
s	saturation
tp	two-phase
w	wall

1. Introduction

Dispersed flow is a typical flow pattern of film boiling characterized by liquid droplets entrained in a continuous flowing vapor. Heat transfer of the dispersed flow is of particular importance in steam generating systems, in metallurgical apparatus, and in nuclear reactor systems under a hypothetical loss-of-coolant accident.

On principle, heat in this regime can be removed from the surface basically by three paths, namely, droplet-wall impact heat transfer, vapor convective heat transfer and radiation heat transfer. For most post-dryout conditions, wall temperature usually exceeds the Leidenfrost temperature. Only a few droplets in these cases are able to touch or come near the heated wall. During impingement, they extract a very limited amount of energy, usually less than 5% [1, 2]. Vapor convection thus becomes the dominant path of heat transfer to the wall. Based on this consideration, current models of dispersed flow heat transfer, both empirical [3] and phenomenological [1], reasonably introduced the traditional correlation of single phase convection, such as the Dittus-Boelter correlation, with modifications to account for two-phase effects. Certain degree of success has been reported using these models to predict the wall temperatures along the straight channel in post-dryout regime in spite of some uncertainties on other predicted parameters, such as the vapor superheat [5].

For curved single phase and two phase flows, numerical and experimental studies have revealed a significant departure of fluid dynamics and heat transfer characteristics from those of the flows in straight channels. In the curved channel the flow and the heat transfer are essentially three dimensional due to the occurrence of the centrifugal forces and the induced cross-stream flows, *i.e.* the secondary flows. Rowe [5], Patankar *et al.* [6] studied experimentally and numerically the turbulent flow field in a 180 deg bend at the radius ratio of $R_c/R_t = 24$, and Reynolds number $Re = 2.36 \times 10^5$. The flow was found to be accelerated in the outer side, and decelerated in the inner side of the bend. In the cross-section, a secondary flow was found to increase gradually from bend inlet to a maximum at about 30 deg and then decrease to a steady value past 90 deg.

In addition to the change of velocity field, distribution of fluid temperature was also experimentally confirmed to be changed with the maximum temperature shifted to the inner side of the bend [7]. Local heat transfer coefficients at the outer side are therefore larger than those at the inner side of the bend [8]. For two-phase flows, an additional important parameter influenced by the curvature is the void fraction. Gardner & Nell [9] measured the void distribution of air-water adiabatic flow in vertical 90 deg bends. They showed that the gravitational effect worked only at the modified Froude number $Fr = V_m^2/(gR_c \sin\beta)$ less than one. For other regions, water was always centrifugally driven to the outer side of the bend. Davis & Hoang [10] observed also the phase separation phenomenon in a vertical 180 deg bend. A high percentage of water was observed at the outer side of the bend soon after the bend inlet. For dispersed flow boiling in the bend, Lautenschlager [11] revealed that the two-phase structural change can bring about significant heat transfer augmentation compared with the vertical flow. To arrive a better understanding of the heat transfer mechanisms, however, substantial information is needed on the behaviors of the phase distribution.

In view of the previous investigations, especially the work of Lautenschlager [11], this paper provides a further study on the heat transfer mechanisms of the dispersed flow based on the extensive measurements of phase distribution. Experiments were carried out with refrigerant R12 as modeling fluid at mass flow rates (G) 400, 680, 1240, 2000 kg/m^{2}s, critical pressure ratios (P/P_{cr}) 0.23, 0.46, 0.7, wall heat fluxes ($\dot{q}_w$) 20, 30, 40, 50, 60 kW/m^2, bend inlet equilibrium qualities ($x_{i,e}$) 0.47 - 1.09, and ratios of bend and tube radii (R_c/R_t) 28, 42. Local liquid concentration was measured by an impedance void-meter over five different regions of the cross-section and at bend angular positions (β) $15°, 30°, 60°$ for $R_c/R_t = 28$, and $0°, 15°, 45°, 90°$ for $R_c/R_t = 42$.

2. Experimental Apparatus & Procedure

The two-phase flow experimental loop is shown schematically in Figure 1, and has been described elsewhere [11, 19] in detail.

By regulating the heating power of the preheater and the evaporator, two-phase annular flow of refrigerant R-12 was formed at the beginning of the test section. The whole test section consisted of two straight tubes and a vertical 90 deg bend. The inner diameter of the test section was 28.5 mm. The ellipticity along the bend was less than 4 % and maximum deviation in wall thickness after bending was about 4.6 %. The test section was made of stainless steel, and was heated by direct current. 60 chromel-alumel thermocouples, 0.5 mm in diameter, were installed on the outer surface of the pipe. To obtain a developed pattern of the dispersed flow, dryout was regulated to occur 2.5 m upstream from the bend inlet. The layout of the test section is shown in figure 2.

A specially developed impedance void-meter was installed along the bend (see also figure 2). It was used to measure the local droplet concentration in axial direction and in five regions of the cross-section, namely, the outer region that is close to the outer wall, the side region, the core region and the inner region that is close to the inner wall.

Figure 3 shows the structure of the void-meter. It was composed of thin concentric rings that were divided and wired together to constitute five separate capacitors in the cross-section. Supplied with high frequency voltage, these capacitors were measured by a digital capacitance meter Model 72BD which had a precision of less than 0.15% of readings.

The principle of the void-meter lies on the fact that the impedance between two electrodes immersed in a two-phase flow depends upon the void fraction and the flow pattern. Under the dispersed droplet flow conditions, the relationship between the droplet concentration $1-\alpha$, and the permittivity, or the dielectric constant ε of the flow was theoretically analyzed and given as Maxwell law [12]

$$1-\alpha = \frac{\varepsilon_{tp}-\varepsilon_g}{\varepsilon_{tp}+2\varepsilon_g}\frac{\varepsilon_f+2\varepsilon_g}{\varepsilon_f-\varepsilon_g}$$

under the assumptions of homogenous field between electrodes, and large interval among droplets compared to their dimensions. Cimorelli and Evangelisti [13] indicated from their study of the impedance void-meter in bulk boiling conditions, that as long as the Maxwell assumptions were satisfied, the difference between the reference value and the measured value was much smaller than 0.02 for dispersed flow.

Nevertheless, uncertainty may exist if dispersed flow forms a thin liquid film on one of the electrodes due to the droplets impingement. In this case, the total capacitance measured is actually the resultant of the two capacitors in series, *i.e.* one formed by the liquid film, another by the mixture. The measuring error induced by the formation of liquid film can then be estimated so long as the thickness of the film is known. In view of the superheating state of the vapor, and the high value of the overall void fraction, one can reasonably assume that the film thick is small. This point has already been confirmed by the film thickness measurement of spray cooling [14]. Assuming only 5 % of liquid forms film on the electrode, a rough calculation indicated that the relative error in using Maxwell law is less than 5 %, which is acceptable in this study.

3. Experimental Results & Discussions

3.1 Behaviors of Phase Distribution

One of the typical measurements on phase distribution in the 90 deg vertical bend is shown in figure 4.

Similar to the behavior of the velocity and temperature distributions, a significant non-symmetric phase distribution develops along the bend. Except for low flow velocities, centrifugal forces accelerate the dispersed flow in the outer side, shifting the maximum droplet concentration from center to the outer. This kind of phase separation begins at the bend inlet, and prevails along the first 45 deg bend region.

Liquid reversal from the outer region to the inner region produced by the pressure gradient and the interfacial forces becomes noticeable in the later part of the bend. As seen from the same figure, liquid fraction increases both in the side and the inner regions while it decreases in the outer region. Droplet concentration in the core region, however, remains nearly unchanged in this part. This reveals that the secondary liquid reversal is restricted only to the boundary layer near the wall.

In the following, a phase distribution factor F_i is employed to study the parametric influences on the phase separation and redistribution. It is defined as $F_i = (1-\alpha)_i A_i / (\sum_k (1-\alpha)_k A_k)$, which gives a relative magnitude of liquid concentration in region i over the whole cross-section.

Influence of inlet velocity

The process of the phase separation and redistribution depends critically on the mass flow rate, or the inlet mean velocity $V_m = G/(\alpha\varrho_g + (1-\alpha)\varrho_f)$ which is closely connected with the magnitude of the centrifugal force and the secondary flow. As clearly shown in figure 5, increasing the inlet velocity, more liquid droplets are transported towards outside. Such phase separation behavior extends even to the bend inlet. For the same reason, at higher inlet velocity, liquid reversal towards inner side increases more significantly along the bend. At $V_m = 18.8$ m/s, a liquid film is formed in the circumference near the bend outlet.

Influence of bend radius

With the same inlet velocity, however, the phase distribution can exhibit different characters for different bends. Figure 6 shows the influence of bend radius, or, the Dean number $De = Re\sqrt{R_t/R_c} = (GxD/\mu_g\alpha)\sqrt{R_t/R_c}$, that describes the relative importance of the inertia and centrifugal forces to the viscous force. In the small radius bend, the degree of phase separation is more serious in the first half bend due to the centrifugal effects. In addition, the increase of the pressure gradient makes the liquid in the boundary layer more easier to be transported towards inner side. As a result, liquid inward circulation is much faster in the small radius bend than that in the large radius bend.

Influence of Fr number

Usually the inertia and the centrifugal forces are so strong that the gravitational effect can be neglected. Under these flow conditions, the value of modified Froude number $Fr = V_m^2/(gR_c sin\beta)$ is much higher than unity. However, for small inlet velocity, the influence of gravity on phase distribution should be considered, especially in the later part of the bend. Figure 7 indicates that the phase distribution is very sensitive to the Froude number when it reaches the value near unity. When the Froude number is less than unity, the gravitational forces can overcome the centrifugal forces in the cross-section, and drive the liquid falling down to the inner side of the bend.

Influence of heat flux

Another factor effecting the phase distribution is the status of balance between the centrifugal and the evaporation-induced forces imposed on the liquid droplets. Governed by the temperature gradient of vapor, a so-called reaction force formed by non-uniform evaporation of individual droplet [15] may counteract the centrifugal effect in the boundary layer. So long as the temperature gradient, or the wall heat flux is not sufficiently high, as the cases of wall heat flux smaller than 60 kW/m^2 in figure 8, the influence of centrifugal forces is dominant, and the phase distribution exhibits the behaviors as discussed above. Once the wall heat flux is high enough, for example over 60 kW/m^2 in the same figure, the reaction forces can reject the droplets from entering into the boundary layer where the pressure gradient prevails. Few droplets are then able to be transported to the inner side.

3.2. Analysis of the Heat Transfer Mechanisms

As the result of phase redistribution, contributions of vapor convection and droplet-wall impact to the wall heat transfer could be tremendously altered in the bend.

Fundamentally speaking, the vapor convection could be influenced by two factors. One is the change of the bulk velocity field in the bend, which results an increase in Nusselt number to be about 20 to 30% above the straight-tube values for single phase flow [8]. Another is the change of local turbulence modulated by droplet addition. Hetsroni [16] showed from measurements that when particle Reynolds Re_p number exceeds a critical value of 400, turbulence is enhanced by vortex shedding. The influence of local turbulence change on vapor convection has been confirmed from the experiment of Choi & Yao [17]. Since the

bend brings about serious phase separation because of the density difference, the slip between the droplet and the vapor phase increases rapidly, which may result in a strong modulation of the local turbulence and the change of vapor convection.

Droplet-wall impact could also play an important role to the wall heat transfer. In the vertical flow, droplet deposition is mainly governed by the turbulent diffusion of continuous vapor phase [18]. Few droplets in this case can attain sufficient kinetics to impact on the heated wall. In the curved flow, however, a simplified calculation [19] indicated that the normal impact velocity of droplets can be at least one order magnitude larger than that in vertical channels [20]. Provided a sufficient deposition rate, droplets could extract a great amount of energy from the surface during the impingement process.

In view of the heat transfer performance of the dispersed flow, two different patterns of heat transfer are distinguished from current measurements.

Non-rewetting heat transfer

Figure 9 presents typical results of the first pattern, namely the "non-rewetting" heat transfer. Under such conditions, the heated wall maintains high values of temperature, usually larger than the Leidendrost temperature. Wetting of liquid droplets on the surface is therefore no longer possible.

In the outer wall region, corresponding to the increase of droplet concentration, a higher value of heat transfer coefficient is measured compared with the value in vertical flow [11]. This is attributed, as discussed above, to the increase of the vapor convection due to the bulk vapor acceleration and local turbulence enhancement by vortex shedding. In addition, droplet-wall impact heat transfer, though "dry" in nature, is also reinforced by the increase of deposition rate indicated by the phase distribution measurement. As droplet concentration decreases in the later part of the bend due to the evaporation and inward reversal, both local turbulence and droplet-wall impact heat transfer are weakened leading to a drop of the heat transfer coefficient and an increase of the wall temperature.

To study the relative importance of each contribution to the total wall heat transfer, evaluation of heat transfer coefficient is made using the correlations recommended in literature and the current experimental data. As seen from the second picture of figure 9, heat transfer coefficient anticipated by the single phase correlation of Moshifeghian [21] is much smaller than the measured one. This indicates that contribution of droplet-wall impact together with the droplet modulation on vapor convection is more important than the change of the bulk flow structure of the vapor.

Heat transfer over the inner wall region on the other hand deteriorates at first as the consequence of the liquid deficiency and flow deceleration. It is then improved somewhat by secondary reversal of the cooled vapor and a few droplets. As droplets evaporate and heat transfer at the outer wall deteriorates in the later part of the bend, heat transfer coefficient decreases again.

It should be noted that even with a proper modification of the heat transfer correlation, for example, the Groneveld-Delorme correlation [3], the predicted results (see curve $h_w(2)$ in the second picture of figure 2) still fail to give the correct magnitude of heat transfer coefficient for the outer wall. This indicates that the traditional correlations have not well included the effect of droplet-wall interaction.

Rewetting heat transfer

Once the droplet deposition rate increases to a certain extent, the amount of heat extracted by droplet dry impact can be large enough to cause the surface temperature to drop to the values near or below the Leidenfrost temperature. Provided a further increase of the deposition rate, stable "wet" collisions of droplets on the heated wall can be maintained. The pattern of rewetting heat transfer is then formed. From appearance, it is characterized by a stable wall temperature near the saturation temperature.

Rewetting heat transfer is usually observed at high and intermediate mass flow rates, large density difference between the phases which means low pressure, and with heat fluxes not too far beyond the critical heat flux. Figure 10 shows one of the typical measurements of this heat transfer pattern.

As seen from the figure, the first position of rewetting usually occurs quite early on the outer wall of about 10 to 30 deg from bend inlet. This position corresponds to the region of maximum positive gradient of droplet concentration. A steep increase of heat transfer coefficient is observed in the outer region with the magnitude close to the one in force convective boiling. This confirms from another aspect the conclusion arrived in phase distribution measurements that a liquid film exits on the outer wall. In the later part of the bend, due to the boiling and inward stretch of liquid film, the liquid fraction decreases and the heat transfer deteriorates somewhat.

Heat transfer at the inner wall decreases at first as a result of liquid deficiency indicated in this figure. After a certain axial distance, however, a turn around point is observed along the temperature curve coincided with the increase of droplet concentration. It indicates the arrival of liquid film in the inner side. Heat transfer is thus significantly enhanced in this region.

4. Conclusions

Current experiments of dispersed flow in vertical bends confirm a significant departure of phase distribution and heat transfer characteristics from the vertical flow. Phase separation develops early from bend inlet and results in a non-symmetric liquid distribution long the bend with the maximum concentration shifted to the outer wall region in most cases. Secondary inward flow is appreciably observed in the later part of the bend and is confined mainly to the boundary region. Among the various parameters, inlet mean velocity and the wall heat flux are the key factors influencing the process of two-phase separation and inward redistribution. The change of phase distribution greatly reinforce the contributions of droplet-wall interaction to the wall heat transfer. By droplet impingement or even forced convective boiling of liquid film in some cases, heat transfer is remarkably augmented, especially at intermediate to large mass fluxes and large density differences.

References

[1] F. Varone Jr. and W.M. Rohsenow (1986): "Post-dryout heat transfer prediction", *Nucl. Eng. & Design*, Vol. 95, pp. 315-327.

[2] T.F. Lin, J.F. Jou and C.H. Hwang (1989): "Turbulent forced convective heat transfer in two-phase evaporating droplet flow through a vertical pipe", *Int. J. Multiphase Flow*, Vol. 15, pp. 997-1009.

[3] D.C. Groneveld and G.G.J. Delorme (1976): "Prediction of thermal non-equilibrium in the post-dryout regime", *Nucl. Eng. Design*, Vol. 36, pp. 17-26.

[4] D. Swinnerton, K.G. Pearson and M.L. Hood (1988): "Steady state post dryout experiments at low quality and medium pressure", *AEEW-R2192.*

[5] M. Rowe (1970): "Measurements and computations of flow in pipe bends," *J. Fluid Mechanics*, Vol. 43, part 4, pp. 771-783.

[6] S.V. Patankar, V.S. Pratap and D.B. Spalding (1975): "Prediction of turbulent flow in curved pipes", *J. Fluid Mechanics*, Vol. 67, part 3, pp. 583-595.

[7] Y. Mori and W. Nakayama (1967): "Study on forced convective heat transfer in curved pipes", *Int. J. Heat Mass Transfer*, Vol. 10, pp. 37-59.

[8] S.D.-Joshi and R.K. Shah (1986): "Convective heat transfer in bends and fittings", *Handbook of Single-Phase Convective Heat Transfer*, Chapter 10, Editors: S. Kakac, R.K. Shah, W. Aung, John Wiley & Sons, New York.

[9] G.C. Gardner and P.H. Neller (1970): "Phase distributions in flow of an air water mixture round bends and past obstructions", *Proc. Inst. Mech. Eng.*, Vol. 184, No. 3C, pp. 93-101.

[10] K. Hoang and M.R. Davis (1980): "The influence of return bends on velocity ratio in gas-liquid pipe flow", *Int. J. Multiphase Flow*, Vol. 6, pp. 267-272.

[11] G. Lautenschlager (1988): "Wärmeübergang in Krümmern bei Sprühkühlung, *Dissertation*, Technical University of Munich.

[12] G.F. Hewitt (1978): *Measurement of two phase flow parameters*, Acadamic press, London.

[13] L. Cimorelli and R. Evangelisti (1967): "The application of the capacitance method for void fraction measurement in the bulk boiling conditions", *Int. J. Heat Mass Transfer*, Vol. 10, pp. 277-288.

[14] L. Bolle and J.C. Moureau (1982): "Spray cooling of hot surfaces," *Multiphase Science & Technology*, Vol. 1, Editors: G.F. Hewitt, J.M. Delhaye, N. Zuber, Hemisphere, Washington, D.C..

[15] E.N. Ganic and W.M. Rohsenow (1979): "On the mechanism of liquid drop deposition in two-phase dispersed flow," *J. of Heat Transfer,*, Vol. 101, pp. 288-294.

[16] G. Hetsroni (1989): "Particles-turbulence interaction", *Int. J. Multiphase Flow*, Vol. 15, No.5, pp. 735-746.

[17] K.J. Choi and S.C. Yao (1987): "Mechanisms of film boiling heat transfer of normally impacting spray", *Int. J. Heat Mass Transfer*, Vol. 30, pp. 311-318.

[18] A.H. Govan, G.F. Hewitt and J.W. Terry (1989): "Measurements of particle motion in a turbulent pipe flow using an axial-viewing technique", *Int. Conf. on Mechanics of Two-Phase Flows*, Taipei, China

[19] M.J. Wang and F. Mayinger (1990): "Void fraction and heat transfer of dispersed two-phase flow in 90° circular bends", *European Two-Phase Flow Meeting*, Varese, Italy

[20] B.Y.H. Liu and T.A. Ilori (1974): "Aerosol deposition in turbulent pipe flow", *Environmental Sci. & Tech.*, Vol. 8, pp. 351-356.

[21] M. Moshfeghian and K.J. Bell (1979): "Local heat transfer measurements in and downstream from a U-bend", *ASME Paper*, No. 79-HT-82.

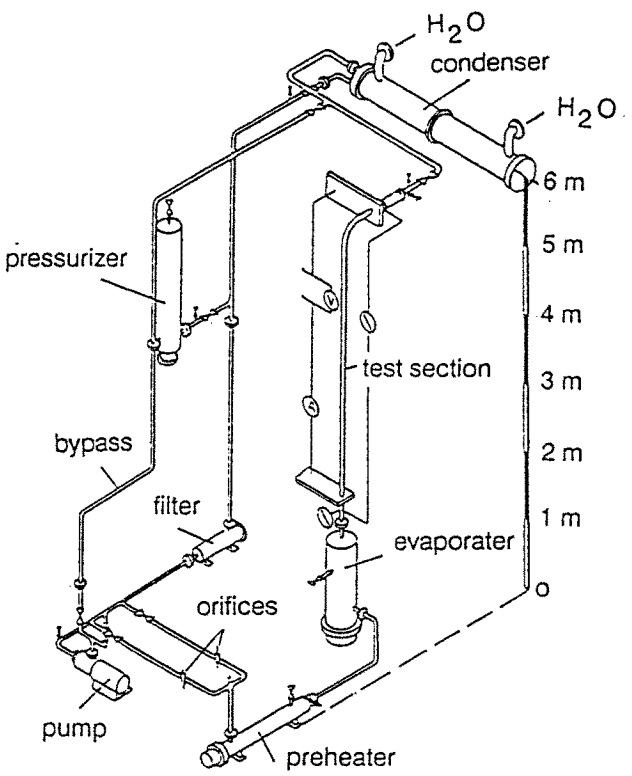

Fig. 1 R-12 experimental loop

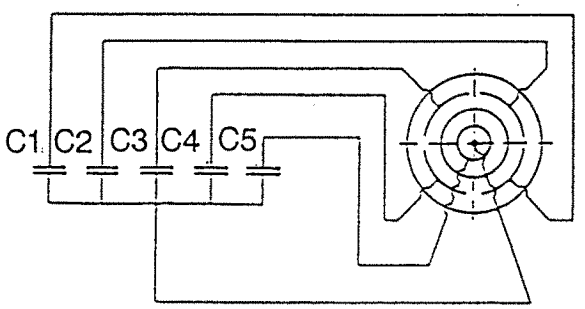

Fig. 3 Structure of impedance void meter

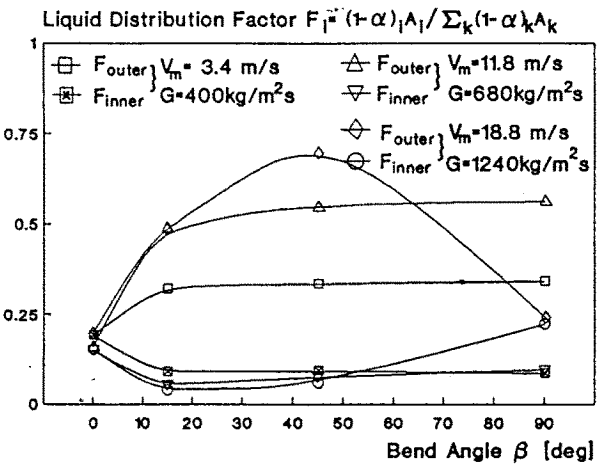

Fig. 5 Influence of inlet velocity on phase distribution (G=400 kg/m^{2}s, $\dot{q}_w$=30 kW/m^2, R_c=0.6 m)

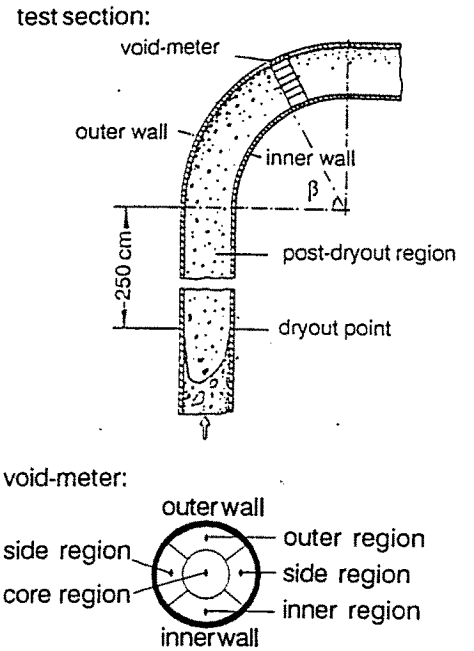

Fig. 2 Layout of test section and void-meter

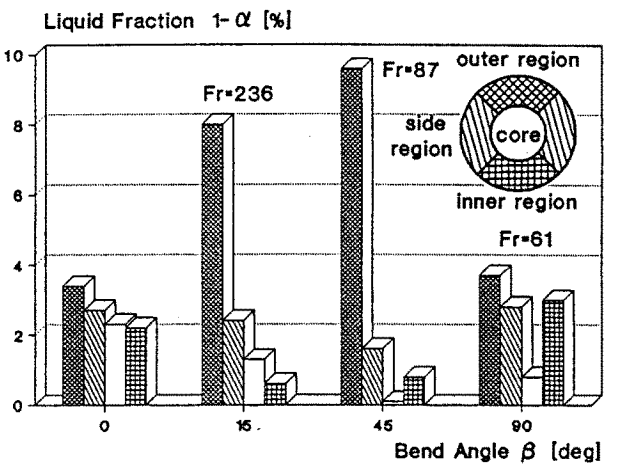

Fig. 4 Phase distribution at R_c=0.6 m, P=9.5 bar, G=1240 kg/m^{2}s, $\dot{q}_w$=30 kW/m^2, $x_{e,i}$ = 0.82

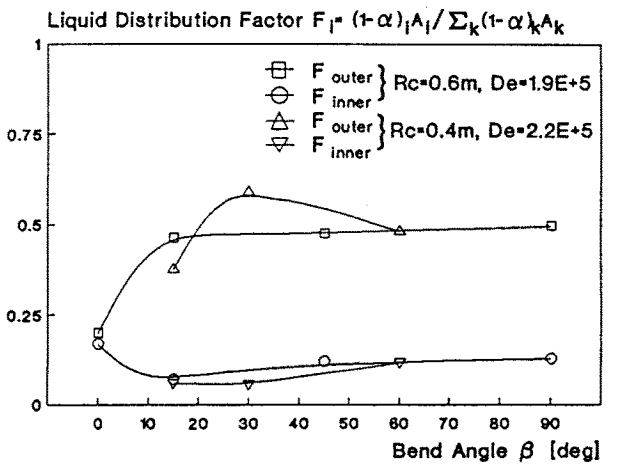

Fig. 6 Influence of bend radius on phase distribution (G=680 kg/m^{2}s, $\dot{q}_w$=20 kW/m^2, P=9.5 bar)

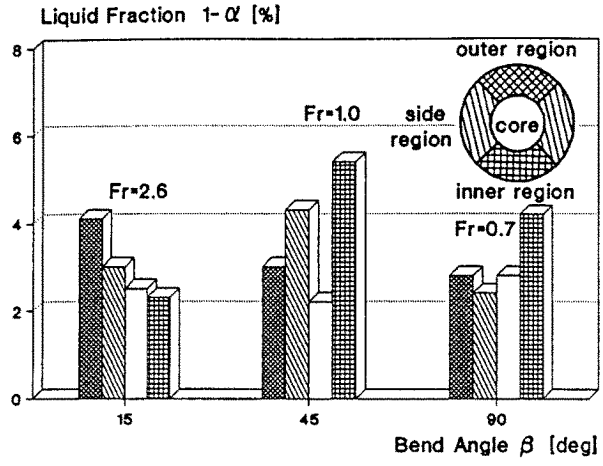

Fig. 7 Influence of Fr number on phase distribution (G=400 kg/m^{2}s, $\dot{q}_w$=20 kW/m^2, P=28.5 bar, R_c=0.6 m, V_m=2.0 m/s)

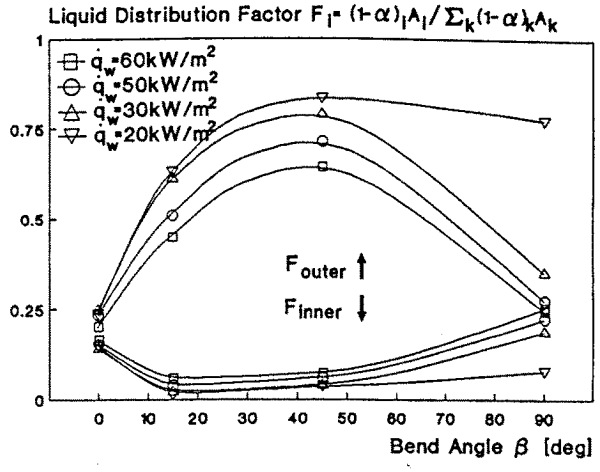

Fig. 8 Influence of heat flux on phase distribution (G=1240 kg/m^{2}s, P=9.5 bar, R_c=0.6 m)

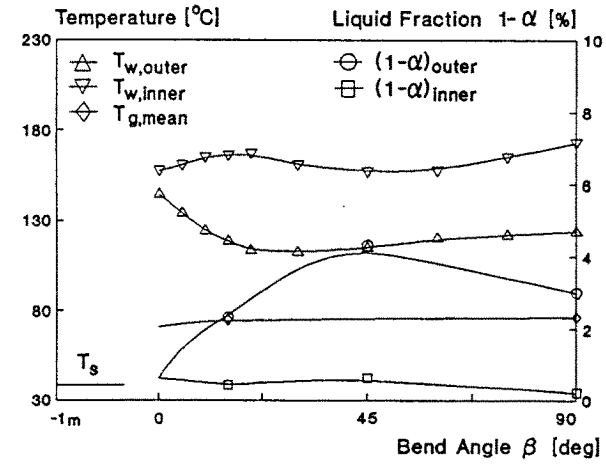

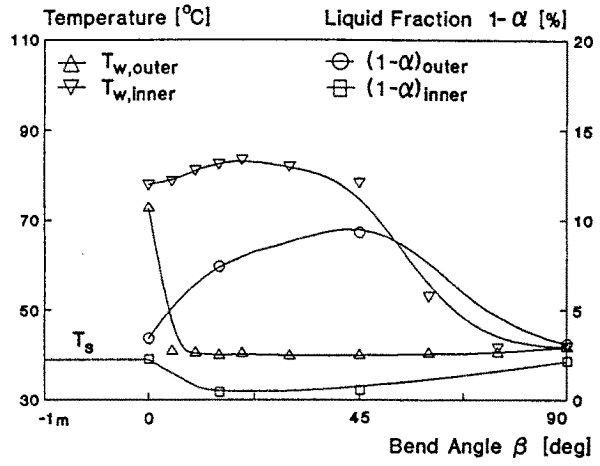

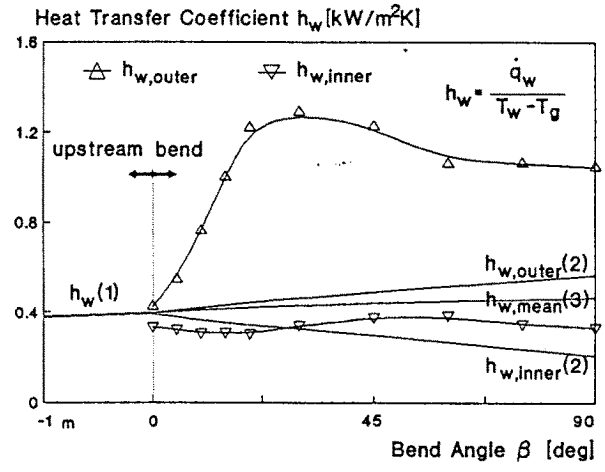

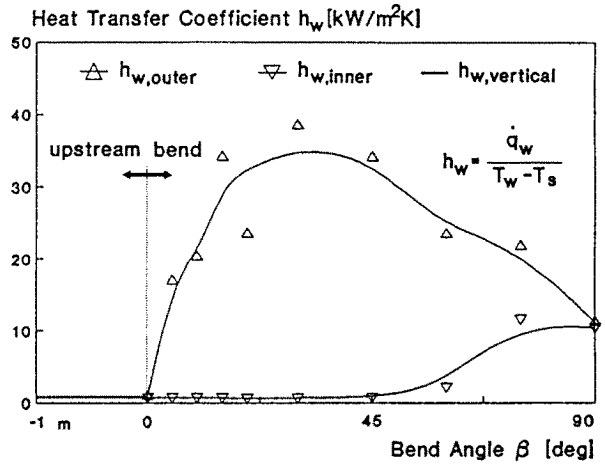

$h_w(1)$: results calculated using the model of [11]
$h_w(2)$: results estimated using the correlation of [3]
$h_w(3)$: results estimated using the correlation of [21]

Fig. 9 Non-rewetting heat transfer at G=400 kg/m^{2}s, P=9.5 bar, $\dot{q}_w$=30 kW/m^2, R_c=0.6 m, $x_{i,e}$ = 1.02

Fig. 10 Rewetting heat transfer at G=1240 kg/m^{2}s, P=9.5 bar, $\dot{q}_w$=30 kW/m^2, R_c=0.6 m, $x_{i,e}$ = 0.82